ORIGINAL PAPER - PRODUCTION ENGINEERING

CrossMark

Co-estimation of saturation functions (k_r and P_c) from unsteady-state core-flood experiment in tight carbonate rocks

Muhammad Yaralidarani[1] · Hamidreza Shahverdi[1]

© The Author(s) 2018

Abstract

The production from oil and gas reservoirs is greatly affected by rock and fluid properties of the porous rock. Capillary pressure (P_c) and relative permeability (k_r) are two important properties employed in the mathematical simulation reservoirs for predicting oil recovery from underground hydrocarbon resources. In this study, various core-flood experiments were performed using different tight carbonate rock samples for oil–water and oil–gas systems. The objective of this research is to investigate the multi-phase flow functions (k_r and P_c) in tight formations. The k_r curves of each sample were obtained by two different mathematical methods: the history-matching (ant colony optimization) technique and analytical method (JBN). The comparison between the relative permeability of the history-matching technique with that of the JBN method revealed a significant discrepancy between them. The modeling of an experiment using k_r of JBN revealed a significant difference between experimental and simulation oil production, whereas the relative permeability of history matching accurately reproduced the experimental oil recovery. This observation highlights the inadequacy of the JBN technique for determination of relative permeability in particular in the tight rock where capillary forces are important. In addition to the relative permeability, the capillary pressure values as a function of saturation were estimated from core-flood tests using a history-matching technique. The comparison between oil–water capillary pressures obtained from centrifuge tests with those of core-flood experiments depicted good agreement, whereas the capillary pressure of oil–gas system measured from core-flood tests was considerably different from centrifuge experiment results. This outcome demonstrated that the capillary pressure obtained from centrifuge experiments in some cases may not be representative of dynamic capillary pressure governing the multi-phase flow in porous media.

Keywords Relative permeability · Capillary pressure · Porous media · Oil · Gas · Water

Introduction

Due to the great importance of relative permeability (k_r) and capillary pressure (P_c) curves for the mathematical modeling of the multi-phase flow in porous media (e.g., petroleum reservoir, carbon dioxide geological storage, and underground water resources), many types of research have been directed toward the prediction of these parameters. Over the past years, various numerical and experimental methods have been developed for the direct measurement and estimation of both k_r and P_c (O'Meara Jr and Lease 1983; Watson et al. 1988; Nordtvedt et al. 1993; Shahverdi et al.

2011; Shahverdi 2012; Pini and Benson 2013). Shahverdi (2012) developed a new method for simultaneous estimation of three-phase k_r and P_c values based on history matching of unsteady-state experimental data using the genetic algorithm. He verified his method by making use of two sets of three-phase experimental data published in the literatures and then applied his methodology to calculate three-phase k_r values of different WAG cycles. Pini and Benson (2013) used three different fluid pairs and measured k_r and P_c drainage curves simultaneously on a single Berea Sandstone core. They proved reliability of the measured k_r curves by comparing their measured data on Berea Sandstone cores and with various gas/liquid pairs and those obtained from the literature obtained.

The most common experimental methods for the measurement of relative permeability are steady-state and unsteady-state experiments. In the steady-state method,

✉ Hamidreza Shahverdi
hr_shahverdi@cc.iut.ac.ir

[1] Department of Chemical Engineering, Isfahan University of Technology, Isfahan 84156-83111, Iran

two immiscible fluids are injected co-currently at a specific ratio through the core until the same production ratios are achieved from the outlet of the core. In this method, the relative permeability values can be calculated directly using Darcy's law. Although a steady-state test facilitates the direct determination of k_r curves, it is a very time-consuming and costly method with some limitations such as neglecting capillary effects, one-dimensional flow in the core, and isothermal and incompressible fluid (Cinar et al. 2007). Moreover, the ratio of the injected fluids is not technically allowed to be less than a certain value, hence the relative permeability at low saturations cannot be measured. An alternative technique for determining the relative permeability values is the unsteady-state method which is much quicker than the steady-state test. In the unsteady-state test, one fluid (which is immiscible with the fluid in the core) is injected through the core to displace the resident fluid inside the core. Then the fluid production and pressure across the core are measured against time. Since the flow in the porous media is occurring under the unsteady-state condition, the relative permeability data cannot be obtained directly from Darcy's equation. Hence, two general methods have been devised for the measurement of relative permeability from unsteady-state tests: the analytical (explicit) method and the optimization (implicit) method. In the analytical method, the Buckley–Leverett theory (Buckley and Leverett 1942) is used to derive the relative permeability from the production and pressure profile (Johnson et al. 1959). However, in the optimization technique, the relative permeability curve is tuned in a simulation–optimization procedure to reach an acceptable match between the laboratory results of fluid production and pressure with the corresponding values calculated by the model (Shahverdi et al. 2011). These methods are described in detail later in this manuscript.

Another experimental method for estimating relative permeability that was first introduced by Purcell (1949) involves using the capillary pressure data. In this method, the porous medium is considered as a bundle of capillary tubes with different diameters that are not connected to each other. Purcell (1949) derived an integral formula representing the relative permeabilities as a function of capillary pressure data. This method was later modified by other researchers (Fatt and Dykstra 1951; Burdine 1953).

In addition to the experimental methods, modeling approaches such as pore-network modeling and empirical correlations have been developed for predicting relative permeability (Rajaram et al. 1997; Laroche and Vizika 2005; Sinha and Wang 2007). In the pore-network modeling approach, the void space of a rock is described as a network of pores connected by the throats. The pores and throats are assigned some idealized geometry and rules are developed to determine the multi-phase fluid configurations and transport in these elements. The rules are combined in

the network to compute effective transport properties on a macroscopic scale some tens of pores across (Blunt et al. 2002). The triumph of pore-scale network models depends strongly upon the quality of representing real pore spaces based on their topographical and geometrical characteristics (Xiong et al. 2016).

Various empirical correlations were developed for predicting two-phase and three-phase relative permeability as a function of fluid saturation (Corey 1954; Hirasaki 1973; Sigmund and McCaffery 1979; Honarpour et al. 1982; Chierici 1984; Lomeland et al. 2005; Shahverdi and Sohrabi 2013; Shahverdi and Sohrabi 2014). These correlations contain some parameters depending on the rock and fluid condition that should be adjusted using experimental data.

The geological specification of the rock is one of the key factors that significantly affect multi-phase flow in porous rocks. Many studies have been directed toward investigations of flow functions (k_r and P_c) in sandstone rocks (Oak 1991; Dana and Skoczylas 1999; Haugen et al. 2014; Krause and Benson 2015; Moghadasi et al. 2015; Kianinejad et al. 2016), while much fewer works have been carried out to investigate k_r in carbonate rocks (Spearing et al.; Schneider and Owens 1970; Sola et al. 2007). In general, the carbonate rocks have complex textures and pore networks with high degrees of heterogeneity, unlike sandstone rocks which are more homogeneous in terms of pore structure. In addition to the above features, the capillary forces play a substantial role in governing the fluid flow in carbonate rocks because they typically have low permeability. Hence capillary pressure should be taken into account in simulation (Roehl and Choquette 2012).

In this study, various core-flood experiments are performed on carbonate rocks (with the order of 1 mD permeability) using the oil–water and oil–gas system in order to investigate the performance of the relative permeability in the very low permeability formations. Different mathematical methods are used to estimate the relative permeability and capillary pressure curves from the core-flood experiments. Then the accuracy of each method is discussed. The capillary pressure curves measured from core-flood experiments are also compared to those obtained from centrifuge tests based on which some conclusions are drawn.

Experiment

In this research, four different carbonate rocks taken from an Iranian oil reservoir have been used to perform the unsteady-state core-flood experiments. The physical properties of the core samples are given in Table 1. As can be seen, the order of the permeability of the rock samples used in this study is around 1 mD which is much less than the permeabilities

Table 1 Rock properties and core dimensions used in the experiments

Property	Core #1	Core #2	Core #3	Core #4
Porosity (%)	16.51	24.16	13.90	11.05
Absolute permeability (mD)	0.676	1.238	0.459	0.3
Connate water saturation (%)	20.48	20.94	16.04	27.59
Core diameter (cm)	3.81	3.81	3.81	3.81
Core length (cm)	5.5	5.5	5.5	5.5

Table 2 Fluid properties used in the core-flood tests (water-flooding and gas injection) at a temperature of 25 °C

Brine viscosity (cp)	Brine density (g/cc)	Brine salinity (g/l)	Oil viscosity (cp)	Oil density (g/cc)	Gas viscosity (cp)
1.4	1.19	200	4.92	0.81	0.0183

found in conventional reservoir rocks. The fluid properties used in the experiments are given in Table 2.

Water injection and gas injection tests were carried out into the cores which were initially saturated with the oil and irreducible water (connate water). The experiments were performed at reservoir conditions and under constant pressure drop across the core; hence, the injection rate varies with time. The individual fluid production from the outlet of the core and the injection rate against the time were recorded as the experimental results. The detailed procedure for the experiments is described below:

1. The core plugs were cleaned with toluene and methanol through a Soxhlet extraction apparatus at 60–70 °C to remove residual hydrocarbons, formation brine, salts and other contaminants. Then they were dried in an oven at 70 °C for 8 h. A helium porosimeter and liquid permeameter were used to measure the porosity and permeability of the core.
2. Each core plug was placed in the core holder and then flooded continuously with brine using a constant pressure pump until the core was fully saturated with the brine. As fluid injection proceeds, brine injection rate is measured at different time steps; if it reaches a stable constant value, the only produced fluid is brine which means the core is fully saturated with brine.
3. Crude oil was injected into the core sample to displace the brine and establish the connate water saturation (S_{wi}) in the core. The oil was injected at the representative fluid velocity in the reservoir and the flooding continued until no further brine was produced, i.e., any remaining water in the core is immobile.
4. The core was aged in the crude oil at the temperature of 65 °C for 15 days to restore reservoir wettability condition.
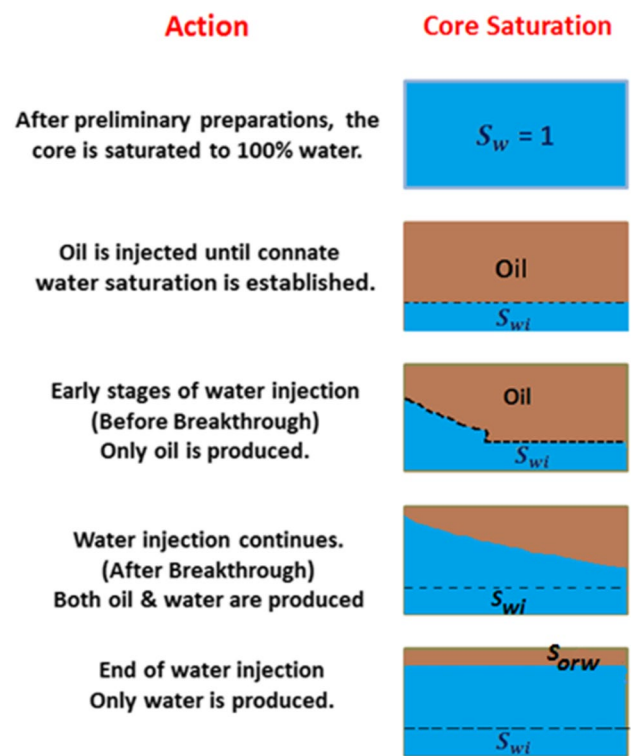

Fig. 1 Schematic of the saturation state in the core for the unsteady-state water-flooding test

Table 3 Initial and boundary conditions used in the core-flood tests (water-flooding and gas injection)

Core number	Initial saturation (%)			Pressure drop (psi)	
	Water	Oil	Gas (nitrogen)	Water injection	Gas injection
1	20.48	79.52	0	165	110
2	20.94	79.06	0	240	100
3	16.04	83.96	0	605	465
4	27.59	72.41	0	1725	1000

5. Water or gas was then injected to displace the oil in the core. The cumulative oil production and fluid injection rates were recorded versus time. The fluid injection continued until no further oil was produced from the core, i.e., residual oil saturation (S_{orw} for water injection test and S_{org} for gas injection test) was attained in the core. It should be noted that during the whole process the pressure drop across the core was held constant.

The schematic of the above procedure and the state of saturation in the core at different stages for the unsteady-state water-flooding are depicted in Fig. 1. It should be noted that a similar process was performed for the gas injection test,

where nitrogen was injected into the core with a constant pressure drop across the core, and the oil production and gas injection rates were recorded during the injection process.

The initial and boundary conditions employed in the experiment are presented in Table 3.

Mathematical method

The most common method for estimating the k_r values from the unsteady-state test is an analytical method that implements the Buckley–Leverett theory (Buckley and Leverett 1942) to derive the relative permeability curve from the results of core-flood test (e.g., production and pressure data). This method was originally devised by Johnson–Bossler–Naumann (Johnson et al. 1959). Later in 1998, (Grader and O'Meara Jr 1988) modified the JBN method to present a more straightforward formulation and procedure for estimating relative permeability curve from the experimental results. In this method, first the saturation of the phase j at the outlet of the core is calculated by the following equation:

$$S_j = S_j^o - R_j + (PV)\frac{dR_j}{d(PV)}, \tag{1}$$

where S_j^o is the initial saturation of phase j, PV is the amount of the injected fluid as a fraction of pore volume, R_j is the fluid production of phase j as a fraction of pore volume, and S_j is the saturation of phase j at the outlet of the core.

Having calculated S_j, the corresponding relative permeability at this saturation can be computed using:

$$k_{rj} = \frac{q_t \mu_j L}{kA} \cdot \frac{f_j}{\Delta P|_{X=1}}, \tag{2}$$

$$\Delta P|_{x=1} = \Delta P - (PV)\frac{d(\Delta P)}{d(PV)}, \tag{3}$$

where k_{rj} is the relative permeability of phase j, q_t is the total production flow rate (cc/h), f_j is the fractional flow of phase j, which is equal to the ratio of q_j to q_t, k is absolute permeability (mD), A is the cross section of the core (cm²), μ_j is the viscosity of phase j (cp), L is the core length (cm), ΔP is the pressure drop across the core (atm), PV is pore volume of the core (cm³).

Despite the simplicity of the JBN method, the formative assumptions of this method (e.g., numerical differentiation error, neglecting the effect of capillary forces and flow in one direction) are very limiting and lead to inaccurate results in many cases. The numerical differentiation of the experimental data (in Eqs. 1–3) can lead to erroneous results, in particular, when the experimental data points are affected by fluctuations. Also ignoring the effect of capillary forces can
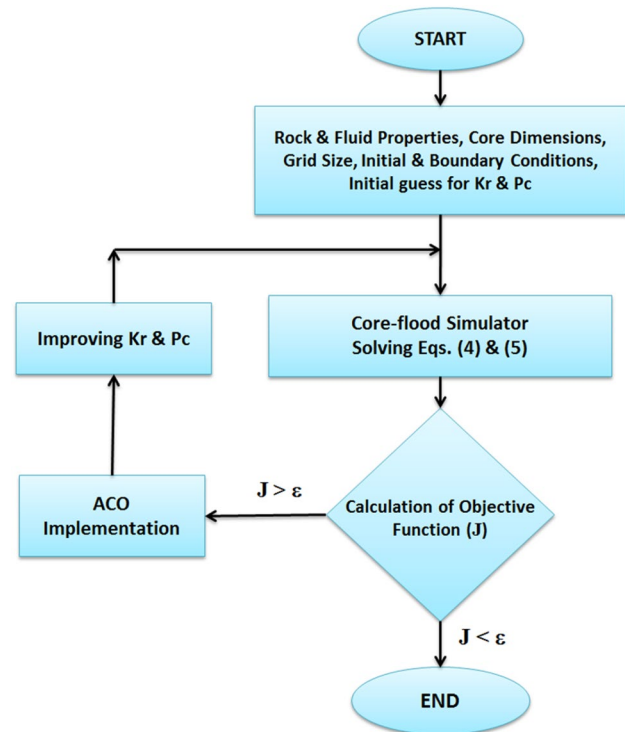

Fig. 2 Estimation of k_r and P_c using ACO optimization technique Reproduced with permission from Yaralidarani and Shahverdi (2016)

result in a significant inaccuracy of the relative permeability data especially for the tight rocks.

A more accurate method for determining of the relative permeability from the unsteady-state test overcoming the aforementioned limitations is the implementation of an optimization technique. In this approach, a relative permeability and capillary pressure model are tuned in an optimization

Table 4 Range of initial guesses for estimating unknown variable in the ACO algorithm for oil–water and gas–oil tests

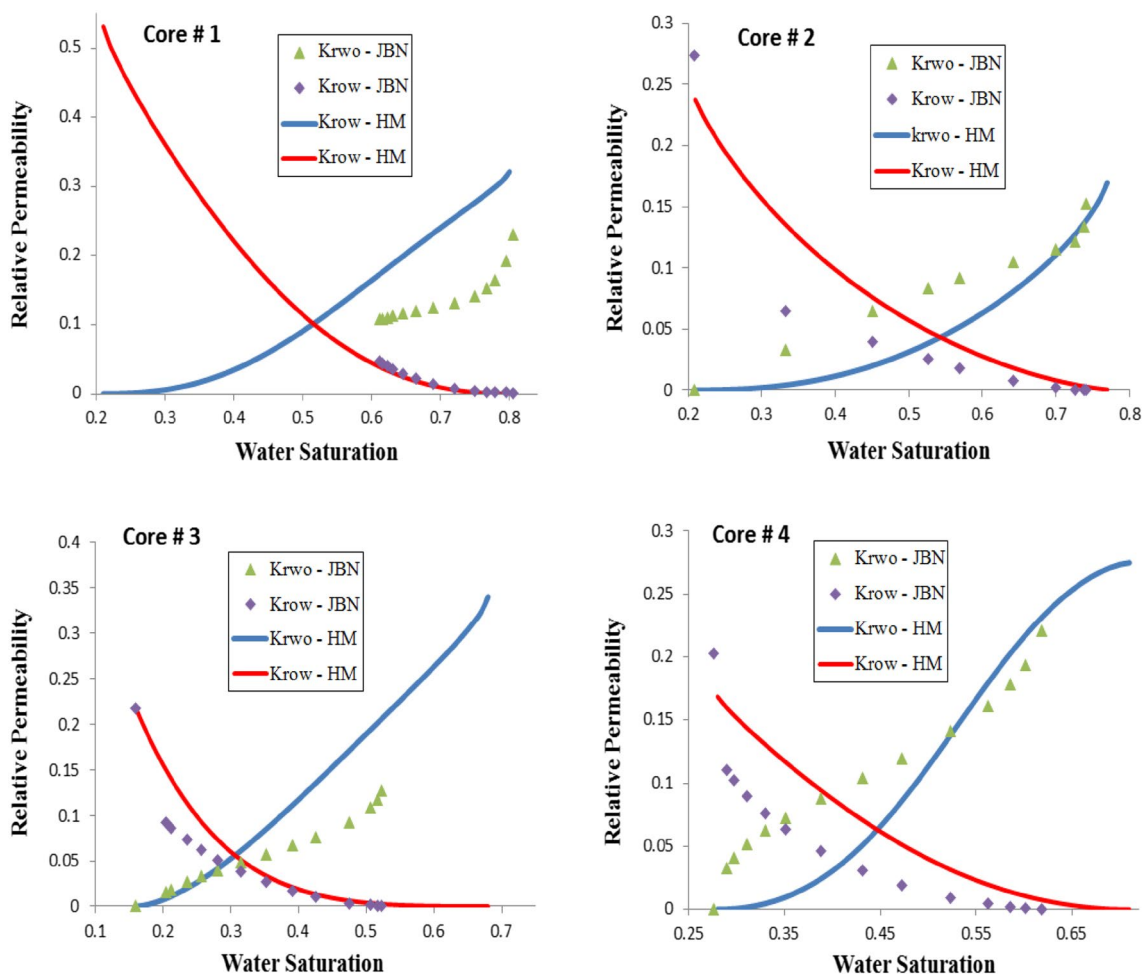| Parameter	Minimum	Maximum	Parameter	Minimum	Maximum
k_{rwo}^o	0.15	0.45	k_{rog}^o	0.25	0.90
L_w	1.0	3.0	L_o	3.0	8.0
E_w	1.0	2.5	E_o	2.0	6.0
T_w	0.5	2.0	T_o	0.5	1.5
S_{orw}	0.15	0.35	S_{org}	0.1	0.2
k_{row}^o	0.10	0.50	k_{rgo}^o	0.10	0.60
L_o	0.50	3.0	L_g	5.0	9.0
E_o	1.5	4.5	E_g	4.0	9.0
T_o	0.8	1.0	T_g	0.6	0.8
c_w	0.0	0.0	c_w	–	–
a_w	0.0	0.0	a_w	–	–
c_o	1.0	125	c_g	4.5	6.0
a_o	0.5	1.5	a_g	1.4	1.6

Fig. 3 Oil and water relative permeability calculated by the history-matching technique (HM) and the analytical method (JBN) for various cores

procedure to reach an acceptable match between the laboratory results of the fluid production, pressure drop and the corresponding values calculated by the model. The algorithm of the optimization technique is given in Fig. 2. Firstly, the rock and fluid properties (i.e., the size of the core, porosity, permeability, fluid density, and viscosity) measured in the laboratory, together with an initial guess for relative permeability and capillary pressure, are used in a core-flood simulator to obtain the fluid production and pressure against time. Having simulated the core, the difference between experimental production, pressure and those of the simulation data are calculated as the objective function. Then an optimization algorithm is used to minimize the objective function by adjusting the unknown parameters (k_r and P_c).

The core-flood simulator in the optimization algorithm (Yaralidarani and Shahverdi 2016) is responsible for simulation of the multi-phase flow in the rock accounting all the governing forces (i.e., capillary, viscous and gravity). The outputs of the simulation are saturation and pressure distribution along the core as well as the fluid production. The mass conservation

law (continuity equation) and Darcy's law are two fundamental equations used in the numerical simulation. For the oil–water system, the set of equations are as follows:

$$\nabla \cdot \left(\frac{\rho_{ws}}{\mu_w B_w} k k_{rwo} \nabla P_w \right) + q_{Sw} = \frac{\partial}{\partial t} \left(\frac{\rho_{ws}}{B_w} \emptyset S_w \right), \quad (4)$$

$$\nabla \cdot \left(\frac{\rho_{os}}{\mu_o B_o} k k_{row} \nabla P_o \right) + q_{So} = \frac{\partial}{\partial t} \left(\frac{\rho_{os}}{B_o} \emptyset S_o \right), \quad (5)$$

where ρ_{ws} is water density (g/cc) at standard condition, μ_w is water viscosity (cp), B_w is water formation volume factor (cc/Scc), k is absolute permeability (mD), k_{rwo} is two-phase water relative permeability, k_{row} is two-phase oil relative permeability, ∇P_w is pressure gradient of water (atm/cm), q_{Sw} is source/sink term related to water at the standard condition (cc/h), $\emptyset$ is porosity, S_w is water saturation, t is time (h), ρ_{wo} is oil density at standard condition (g/cc), μ_o is oil viscosity (cp), B_o is oil formation volume factor (cc/Scc), S_o
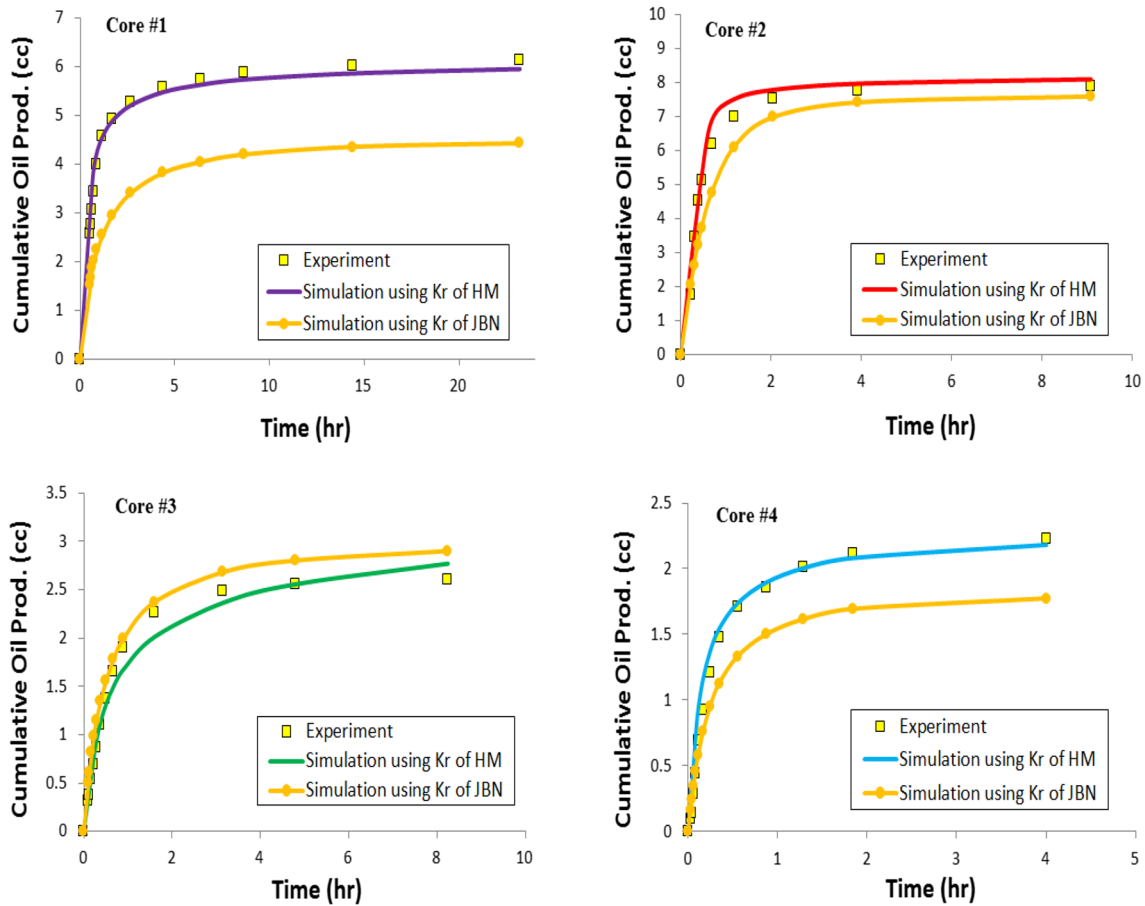
Fig. 4 Experimental results of cumulative oil production compared to the simulation results using k_r of HM and k_r of JBN method

is oil saturation and q_{So} is source/sink term related to water at standard condition.

Capillary pressure is defined as follows:

$$P_{cow} = P_o - P_w, \tag{6}$$

where P_o and P_w are water and oil phase pressure (atm), respectively. In addition to the above equation, considering the definition of saturation leads to the following equation:

$$S_w + S_o = 1. \tag{7}$$

By solving Eqs. (4–7) simultaneously, the unknown variables (e.g., P_o, P_w, S_w, and S_o) and fluid production are obtained. It should be noted that similar equations are employed for the oil–gas system.

In this study, a modified version of the ant colony optimization (ACO) technique is used as an optimization tool in conjunction with a core-flood simulator (as described above) to obtain the relative permeability and capillary pressure simultaneously from the unsteady-state tests (Yaralidarani and Shahverdi 2016).

The aim of the optimization technique presented in Fig. 2 is to obtain the relative permeability and capillary

pressure curves that reproduce a reasonable match of fluid production and pressure with the corresponding experimental data. The objective function (shown in Fig. 2) is defined as follows:

$$J = W_o \frac{1}{\sigma_o^2} \sum_{i=1}^{N} \left(Q_{O_i}^{Exp.} - Q_{O_i}^{Sim.} \right)^2 + W_I \frac{1}{\sigma_I^2} \sum_{i=1}^{N} \left(q_{f,i}^{Exp.} - q_{f,i}^{Sim.} \right)^2. \tag{8}$$

In the above equation, σ_o and σ_I are standard deviations of experimental values of the oil production and fluid injection rates, respectively. These quantities represent the errors associated with the core-flood experiments, which can be obtained by repetition of the experiment. The terms W_o and W_I are weighted coefficients compensating for the magnitude difference between the two quantities (oil production and fluid injection rate). Finally, Q_o represents the oil production and q_f is the fluid injection rate. The proper adjustment of these factors allows us to match fluid production and pressure to the same extent. (Yaralidarani and Shahverdi 2016).

The relative permeability and capillary pressure curves are represented by a flexible model in the optimization
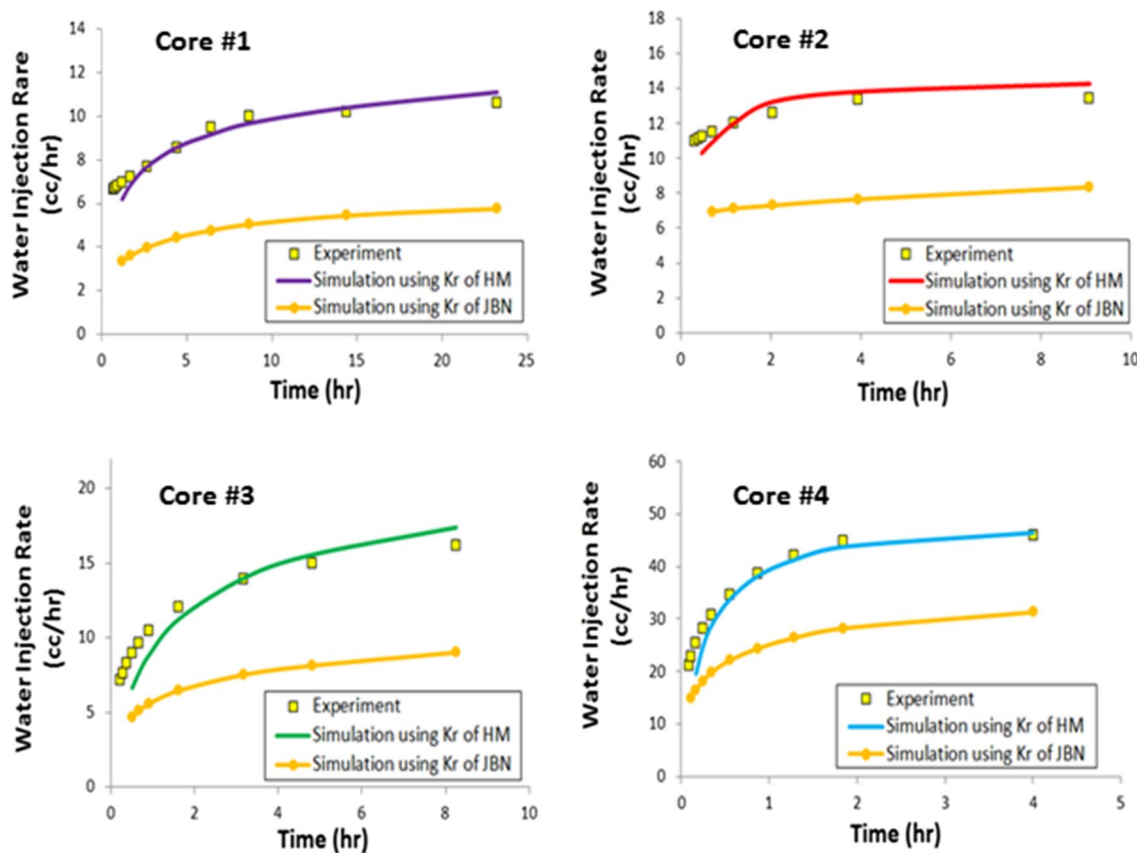
Fig. 5 Experimental results of water injection rate compared to the simulation results using k_r of HM and k_r of JBN method

loop. In this research, the relative permeability and capillary pressure data versus water saturation are produced from the LET model (Eqs. 9–11) (Lomeland et al. 2005) and Skjæveland's model (Eq. 12) (Skjaeveland et al. 1998), respectively.

$$k_{rwo} = k_{rwo}^o \frac{(S_w^*)^{L_w}}{(S_w^*)^{L_w} + E_w (1 - S_w^*)^{T_w}} \qquad (9)$$

$$k_{row} = k_{row}^o \frac{(1 - S_w^*)^{L_o}}{(1 - S_w^*)^{L_o} + E_o(S_w^*)^{T_o}} \qquad (10)$$

$$S_w^* = \frac{S_w - S_{wi}}{1 - S_{wi} - S_{orw}} \qquad (11)$$

$$P_{cow} = \frac{c_w}{\left(\frac{S_w - S_{wi}}{1 - S_{wi}}\right)^{a_w}} - \frac{c_o}{\left(\frac{1 - S_w - S_{orw}}{1 - S_{orw}}\right)^{a_o}}, \qquad (12)$$

where S_w is water saturation, S_o is oil saturation, S_w^* is normalized water saturation, S_{wi} is irreducible water saturation

(connate water), S_{orw} is residual oil saturation, k_{rwo} and k_{row} are water and oil relative permeability in oil–water system, respectively and P_{cow} is oil–water capillary pressure. In Eqs. (9) and (10), parameter T describes the upper part of the curve, L parameter describes the lower part, and parameter E controls the curvature or elevation of the k_r curves. The parameters, k_{rwo}^o and k_{row}^o have physical meaning and represent the maximum two-phase relative permeability of water and oil, respectively. In Eq. (12), c_w and a_w account for the positive part of capillary pressure curve while c_o and a_o control the negative part.

Similarly, LET equations may be used for producing gas–oil relative permeability values. Contrary to the water injection tests which are among imbibition processes, gas injection is a drainage process, and hence gas–oil capillary pressure values are produced using the following equation which is a shortened form of the Skjæveland's capillary pressure model:

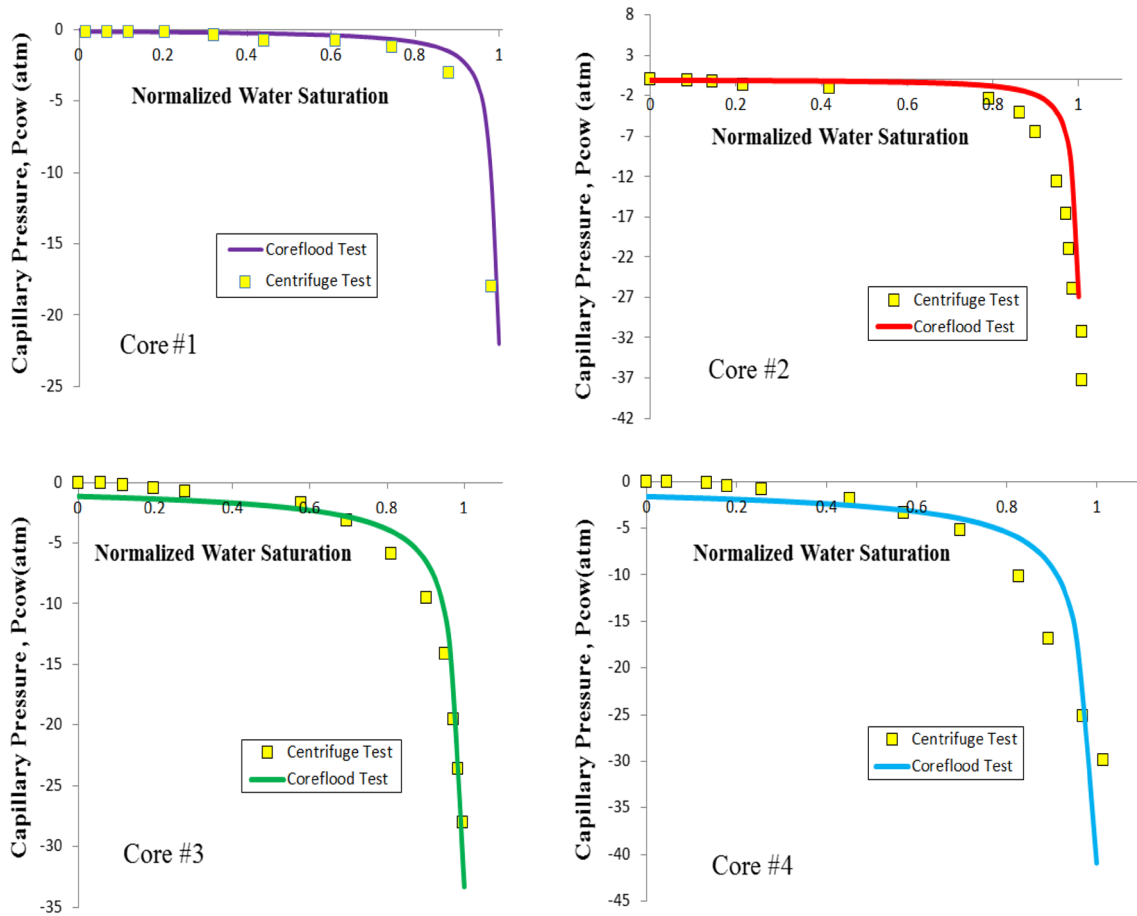$$P_{cgo} = \frac{c_g}{(S_g^*)^{a_g}} \qquad (13)$$

Fig. 6 Oil–water capillary pressure versus normalized water saturation obtained from the centrifuge test and that resulting from history matching of the water injection tests

Table 5 Parameters of the relative permeability (LET) and capillary pressure (Skjæveland) models estimated by history-matching (ACO) technique in water injection test

Parameter	Core #1	Core #2	Core #3	Core #4
Relative permeability (LET)				
K_{rwo}^{o}	0.3680	0.1962	0.3400	0.2750
L_{w}	2.2672	2.1654	1.5512	1.9097
E_{w}	1.3396	1.9139	0.9091	1.1186
T_{w}	0.6793	0.6276	0.7453	1.4497
S_{orw}	0.1970	0.2200	0.3200	0.2900
K_{row}^{o}	0.4173	0.2376	0.2177	0.1686
L_{o}	1.0884	1.3758	2.8709	1.8009
E_{o}	3.0220	2.1939	3.8244	1.6085
T_{o}	0.8402	0.9101	0.9703	0.8947
Capillary pressure (Skjæveland)				
c_{w}	0.0000	0.0000	0.0000	0.0000
a_{w}	0.0000	0.0000	0.0000	0.0000
c_{o}	10.0444	6.0000	95.0000	112.8569
a_{o}	0.8402	1.4043	0.7500	0.7500

$$S_{g}^{*} = \frac{1 - S_{g} - S_{org} - S_{wi}}{1 - S_{org}}, \qquad (14)$$

where S_{g}^{*} is normalized gas saturation, S_{g} is gas saturation, and S_{org} represents residual gas saturation.

The initial and boundary conditions of the model are given in Table 3. The parameters of the relative permeability and capillary pressure model (Eqs. 9–12) are accounted as unknown parameters and the modified ant colony optimization (ACO) algorithm is used to adjust these functions (Yaralidarani and Shahverdi 2016). In other words, the ACO algorithm changes these parameters to obtain an acceptable agreement between experimental data (i.e., cumulative oil production and water injection rate) and those of simulation. Hence, the unknown variables can be represented as the following vector for oil–water tests:

$$S = \left\{ k_{rwo}^{o}, L_{w}, E_{w}, T_{w}, S_{orw}, k_{row}^{o}, L_{o}, E_{o}, T_{o}, c_{w}, a_{w}, c_{o}, a_{o} \right\} \qquad (15)$$

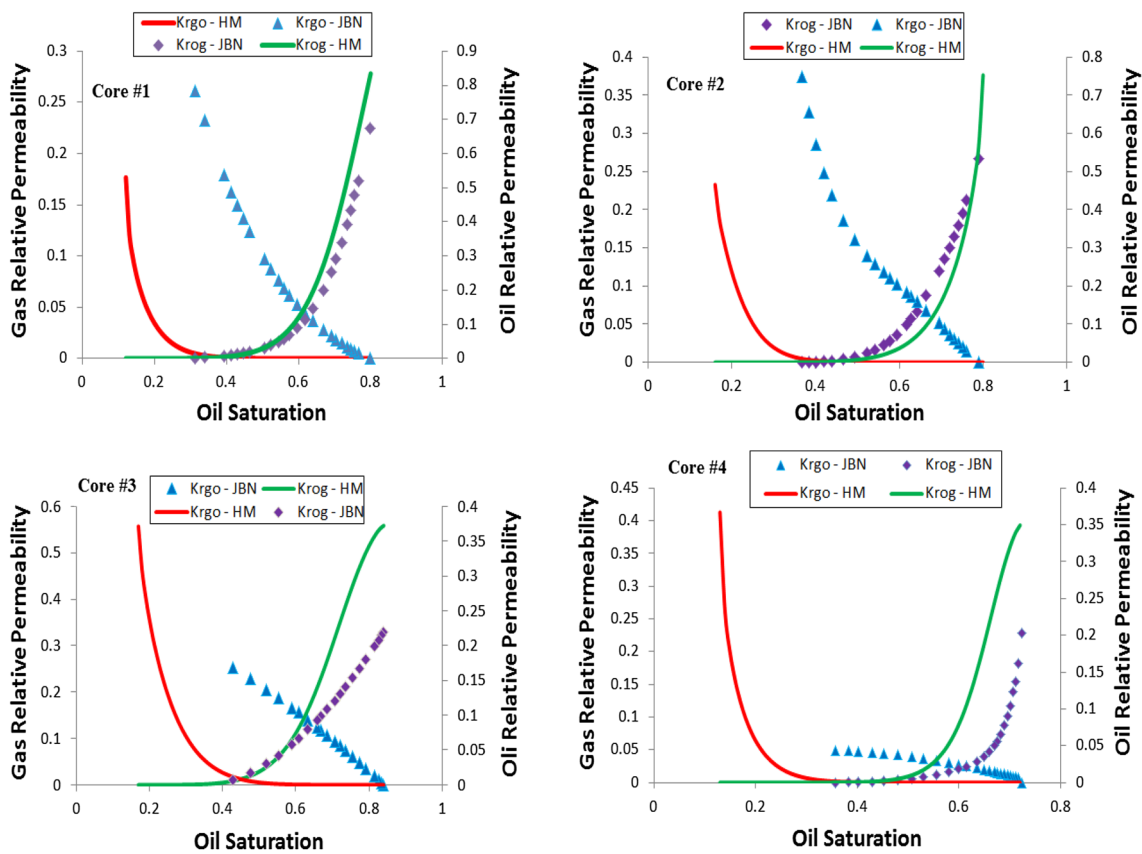and as follows for gas–oil tests:

Fig. 7 Oil and gas relative permeability values versus oil saturation estimated by the history-matching technique (HM) and the analytical method (JBN) for various cores

$$S = \left\{ k^o_{rog}, L_o, E_o, T_o, S_{org}, k^o_{rgo}, L_g, E_g, T_g, c_w, a_w, c_o, a_o \right\}.$$

(16)

Range of initial guesses within which unknown variables are changed automatically by the program to match experimental data is presented in Table 4. It is worth noting that these values have been obtained using sensitivity analysis. It should also be added that 'c_w' and 'a_w' are set equal to zero manually, because they are representative of positive part (spontaneous imbibition) of P_c curve which does not apply to our oil–water experiments. Also note that ending criterion has been defined as 5% discrepancy between the experimental and history-match data.

Results and discussion

(a) *Water injection test*

The experimental results of the water injection tests of different cores (Table 1) were history-matched by the

ACO method as described in the previous section. In this method, the relative permeability and capillary pressure were tuned simultaneously. Also, another set of relative permeability curves were obtained from the water injection test by the JBN technique. The oil–water relative permeabilities versus water saturation obtained from these two methods are presented in Fig. 3. As it was highlighted earlier, the k_r obtained from the history matching is much more realistic than that of the analytical method. The history-matching technique takes into account different kinds of forces (i.e., capillary, viscous and gravity) in the flow calculation, whereas the JBN method ignores the capillary and gravitational forces. The results shown in Fig. 3 depict that the k_r obtained from the JBN method cannot adequately predict the k_r of history matching. This significant disagreement is mainly attributed to the impact of capillary pressure which is pronounced for the tight rocks. This observation is very important because it suggests that the routine approach (JBN method) to deriving the relative permeability curve from the unsteady-state experiments for use in reservoir engineering calculations can produce erroneous results in particular for the tight rocks (carbonate). In addition, JBN method assumes 1D flow and
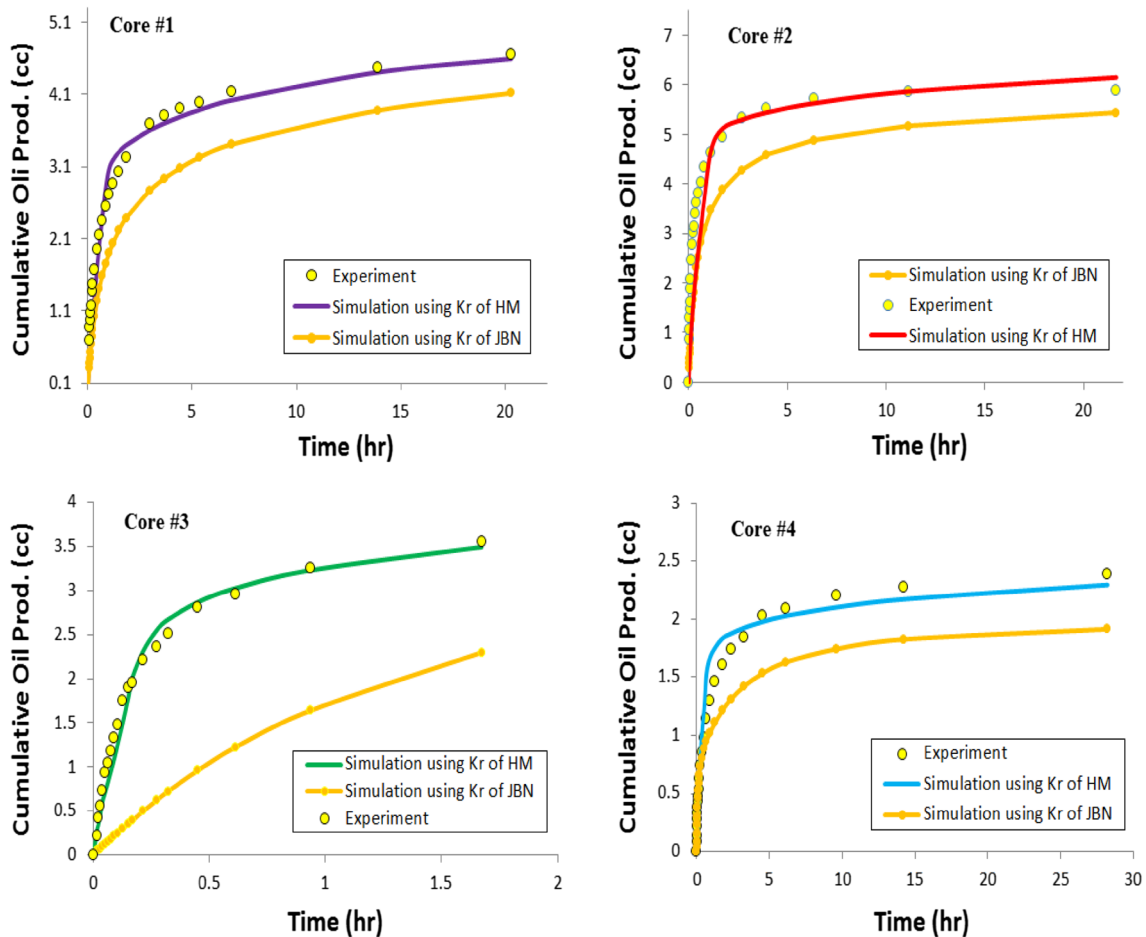
Fig. 8 Experimental results of cumulative oil production compared to the simulation results using k_r of HM and k_r of JBN method

may give incorrect results in case of multi-dimensional flows. Besides, k_r values are calculated by taking numerical derivative of production and pressure data which may cause erroneous results.

The k_r obtained from three-dimensional HM and JBN techniques was employed in the core simulation to reproduce the oil recovery and injection rate of the experiment.

The cumulative oil production, as well as water injection rate versus time obtained from experiment and those resulting from simulation by JBN and HM relative permeability curves, is depicted in Figs. 4 and 5, respectively. As can be seen, using k_r from the JBN method substantially overestimates or underestimates the oil production and injection rates of all experiments. These results confirm the previous conclusion that the JBN method cannot accurately estimate relative permeability from core-flood tests.

The oil–water capillary pressure versus normalized water saturation obtained from centrifuge experiment and

history matching of the water injection test is presented in Fig. 6. As can be seen, there is good agreement between experimental and history-matched P_c curves.

Estimated parameters of the LET relative permeability model and Skjæveland capillary pressure model are provided in Table 5.

(b) *Gas injection test*

Figure 7 shows the relative permeability of the oil–gas system obtained by the history matching (ACO method) and implementation of the JBN technique on the gas injection test. Relative permeabilities in Fig. 7 show large discrepancies between the JBN and HM methods, especially for the gas phase. In order to realize which method (JBN or HM) estimates the relative permeability more accurately, the relative permeability of both techniques was employed in the simulation of gas injection tests to reproduce the oil recovery and injection rate. Figure 8 presents the cumulative oil
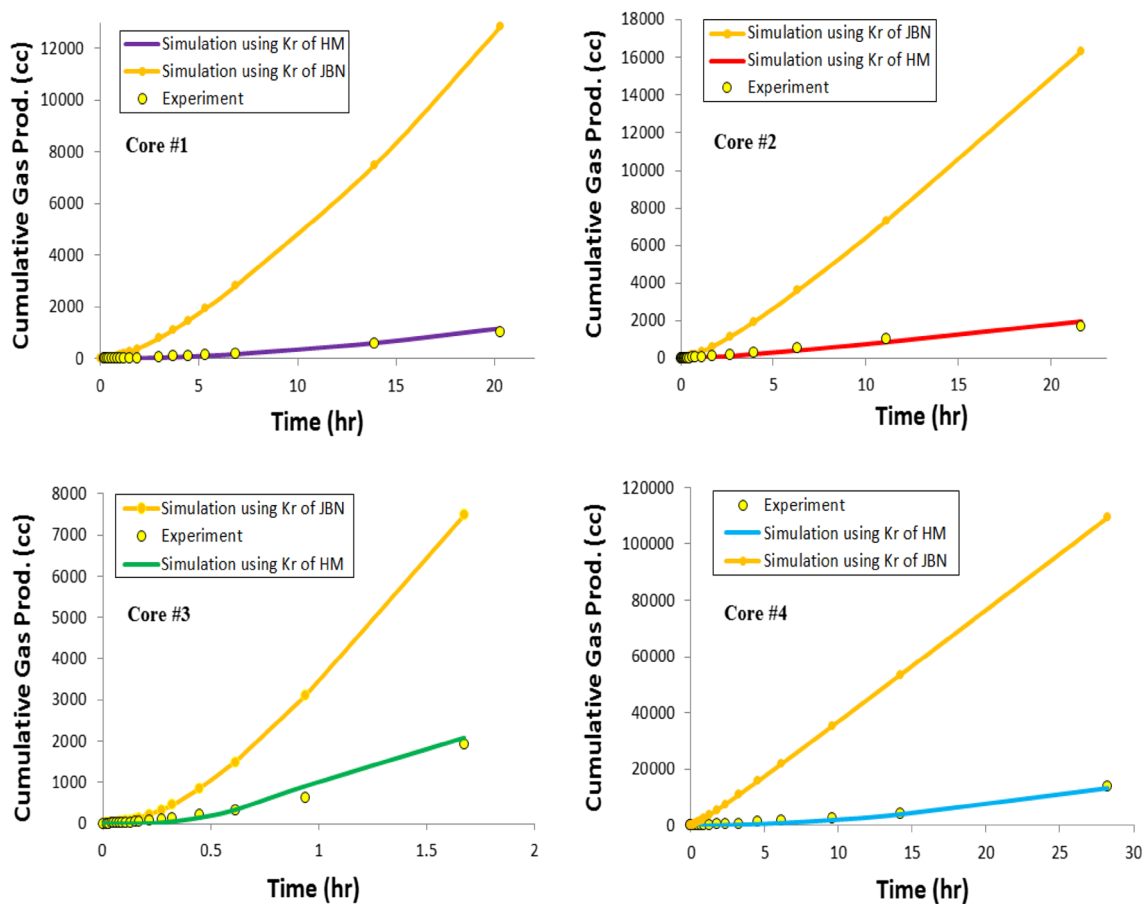
Fig. 9 Experimental results of cumulative gas production compared to the simulation results using k_r of HM and k_r of JBN method

production versus time obtained from the gas injection test and simulations using k_r from the HM and the JBN methods. Figure 9 shows the cumulative gas production versus time obtained from experiment and simulations using k_r from the HM and the JBN methods. As shown in these figures (Figs. 8 and 9), similar to the oil–water system, the simulation results using k_r from the JBN technique are largely different from the experimental results, demonstrating the inaccuracy of the relative permeability data estimated using the JBN technique.

In order to ensure accurate performance of the ACO algorithm, evolution of objective function (Eq. 8) versus iteration number is depicted in Fig. 10 for water injection tests. The declining trend obviously shows that objective function is being minimized meaning a good match between experiment and simulation data is achieved.

These results indicate the significant impact of oil–gas capillary on the relative permeability. In other words, neglecting capillary pressure in the JBN technique leads to the erroneous oil–gas relative permeability curve.

Figure 11 presents the oil–gas capillary pressure versus normalized oil saturation for various cores estimated from

gas injection tests using the history-matching technique and centrifuge experiment. As can be seen, the oil–gas capillary pressure predicted by the history-matching method is considerably different from those of the centrifuge test. This figure illustrates that centrifuge test may not measure the oil–gas capillary pressure precisely. This discrepancy may be attributed to two reasons. First, the centrifuge capillary pressures are measured for an oil–air system and then scaled for the oil–gas system using an interfacial tension (IFT) correction factor. Hence, the scaling of capillary pressure data from air–oil to the oil–gas may be associated with some errors. The second reason is that the capillary pressures of the core-flood test are tuned simultaneously with the relative permeability. In other words, the impact of relative permeability is accounted for in the estimation of capillary pressure from core-flood test, whereas the capillary pressure of the centrifuge test is calculated without consideration for the effect of relative permeability. The authors believe that the capillary pressure of the core-flood test is more representative of the dynamic capillary forces governing flow in the reservoir. Hence, it is advisable for reservoir
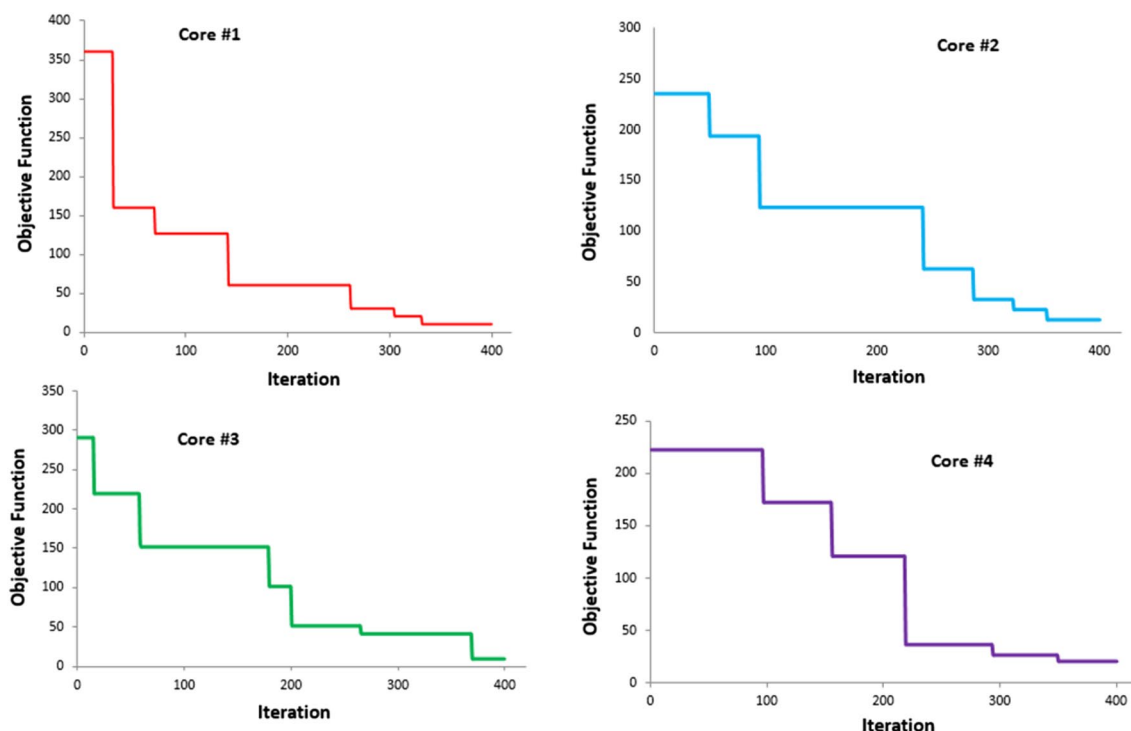
Fig. 10 Variation of objective function versus iteration number for gas–oil tests

engineers to use core-flood capillary pressure for oil reservoir simulations.

The parameters of the LET model, as well as the Skjæveland capillary model, calculated using the history-matching method are provided in Table 6.

Conclusion

The saturation functions (k_r and P_c) were successfully co-estimated from unsteady-state core-flood experiments performed in tight carbonate rocks, using ant colony optimization (ACO) technique. In order to accurately incorporate the physic of the flow, the simulation model was built in three dimensions (X, Y, and Z) with fine grids considering the porosity and permeability distribution (to account for rock heterogeneity). Moreover, the good agreement between

simulation and experimental results was obtained at reasonably low iteration number in optimization technique.

The results depicted that neglecting capillary pressure in core-flood simulation can lead to erroneous relative permeability data. Although adding the capillary pressure function in history-matching process can increase the uncertainty of estimated functions, having an approximate value for P_c (from other tests such centrifuge) as initial guess can modify the estimated k_r and P_c.

The comparison between the results obtained from the analytical method (JBN) and those calculated from the optimization technique revealed significant difference between the two methods. The difference is primarily because the JBN technique ignores the effect of capillary and gravitational forces. In addition to this, the analytical method assumes one-dimensional flow with the
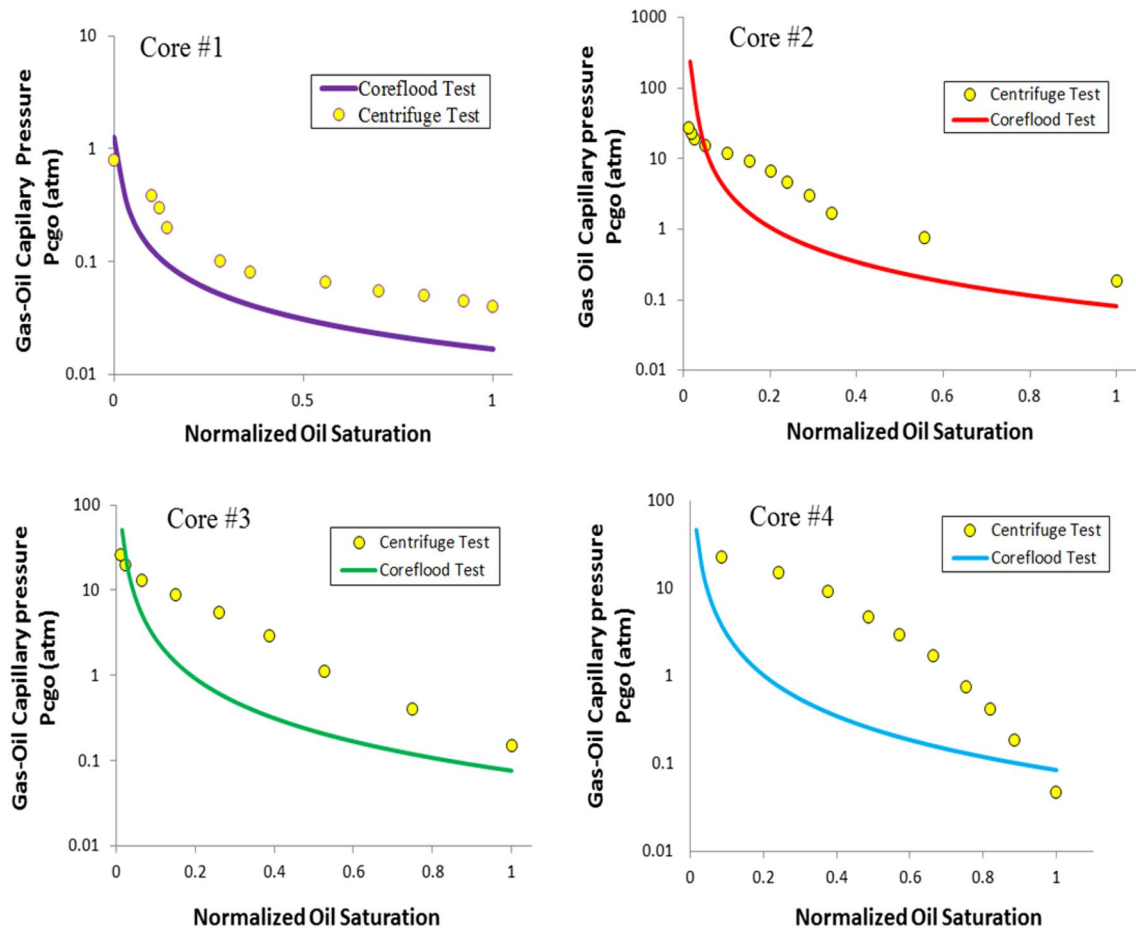
Fig. 11 Oil–gas capillary pressure versus normalized oil saturation obtained from the centrifuge test and those resulting from history matching (HM) of the gas injection tests

Table 6 Parameters of the LET model and the Skjæveland model estimated using the ACO model in a gas injection process considering capillary effects

Parameter	Core #1	Core #2	Core #3	Core #4
Relative permeability (LET)				
K_{rog}^{o}	0.8338	0.7525	0.3725	0.3495
L_o	4.8174	5.6939	4.1173	7.2834
E_o	3.6763	5.1313	2.3899	4.5778
T_o	0.9836	0.6915	1.2738	1.2260
S_{org}	0.1244	0.1549	0.1662	0.1332
K_{rgo}^{o}	0.1766	0.2327	0.5573	0.4130
L_g	7.5538	8.3270	5.3311	8.3836
E_g	6.6417	4.2471	4.9065	8.0087
T_g	0.6596	0.7271	0.7768	0.6771
Capillary pressure (Skjæveland)				
c_g	4.8524	5.3375	5.5456	4.7250
a_g	1.4958	1.5389	1.5468	1.5513

homogeneous rock properties and the constant fluid properties through the core.

The oil–water capillary pressure derived from the core-flood experiment reasonably agreed with that obtained from the centrifuge test, while the capillary pressure of the oil–gas system for the core-flood test was significantly different from the centrifuge test. This has serious implications for reservoir simulation studies that use centrifuge data as simulation inputs.

References

Blunt MJ, Jackson MD, Piri M, Valvatne PH (2002) Detailed physics, predictive capabilities and macroscopic consequences for pore-network models of multiphase flow. Adv Water Resour 25(8):1069–1089

Buckley SE, Leverett M (1942) Mechanism of fluid displacement in sands. Trans AIME 146(01):107–116

Burdine NT (1953) Relative permeability calculations from pore size distribution data. J Petrol Technol 5:71–78. https://doi.org/10.2118/225-G

Chierici GL (1984) Novel relations for drainage and imbibition relative permeabilities. Soc Petrol Eng J 24(03):275–276

Cinar Y, Marquez S, Orr FM (2007) Effect of IFT variation and wettability on three-phase relative permeability. SPE Reservoir Eval Eng 10(03):211–220

Corey AT (1954) The interrelation between gas and oil relative permeabilities. Prod Mon 19(1):38–41

Dana E, Skoczylas F (1999) Gas relative permeability and pore structure of sandstones. Int J Rock Mech Min Sci 36(5):613–625

Fatt I, Dykstra H (1951) Relative permeability studies. J Petrol Technol 3:249–256. https://doi.org/10.2118/951249-G

Grader A, O'Meara Jr D (1988) Dynamic displacement measurements of three-phase relative permeabilities using three immiscible liquids. SPE annual technical conference and exhibition, Society of Petroleum Engineers

Haugen Å, Fernø M, Mason G, Morrow N (2014) Capillary pressure and relative permeability estimated from a single spontaneous imbibition test. J Petrol Sci Eng 115:66–77

Hirasaki G (1973) Estimation of reservoir parameters by history matching oil displacement by water or gas. Shell Oil Co, The Hague

Honarpour M, Koederitz L, Harvey AH (1982) Empirical equations for estimating two-phase relative permeability in consolidated rock. J Petrol Technol 34(12):2905–2908

Johnson EF, Bossler DP, Bossler VON (1959) Calculation of relative permeability from displacement experiments. Society of Petroleum Engineers

Kianinejad A, Chen X, DiCarlo DA (2016) Direct measurement of relative permeability in rocks from unsteady-state saturation profiles. Adv Water Resour 94:1–10

Krause MH, Benson SM (2015) Accurate determination of characteristic relative permeability curves. Adv Water Resour 83:376–388

Laroche C, Vizika O (2005) Two-phase flow properties prediction from small-scale data using pore-network modeling. Transp Porous Media 61(1):77–91

Lomeland F, Ebeltoft E, Thomas WH (2005) A new versatile relative permeability correlation. In: International symposium of the society of core analysts, Toronto, Canada

Moghadasi L, Guadagnini A, Inzoli F, Bartosek M (2015) Interpretation of two-phase relative permeability curves through multiple formulations and Model Quality criteria. J Petrol Sci Eng 135:738–749

Nordtvedt J, Mejia G, Yang P-H, Watson A (1993) Estimation of capillary pressure and relative permeability functions from centrifuge experiments. SPE Reserv Eng 8(04):292–298

Oak M (1991) Three-phase relative permeability of intermediate-wet Berea sandstone. SPE annual technical conference and exhibition. Society of Petroleum Engineers

O'Meara Jr D, Lease W (1983) Multiphase relative permeability measurements using an automated centrifuge. SPE annual technical conference and exhibition. Society of Petroleum Engineers

Pini R, Benson SM (2013) Simultaneous determination of capillary pressure and relative permeability curves from core-flooding experiments with various fluid pairs. Water Resour Res 49(6):3516–3530

Purcell WR (1949) Capillary pressures - their measurement using mercury and the calculation of permeability therefrom. J Petrol Technol 1:39–48. https://doi.org/10.2118/949039-G

Rajaram H, Ferrand LA, Celia MA (1997) Prediction of relative permeabilities for unconsolidated soils using pore-scale network models. Water Resour Res 33(1):43–52

Roehl PO, Choquette PW (2012) Carbonate petroleum reservoirs. Springer, Berlin

Schneider F, Owens W (1970) Sandstone and carbonate two and three-phase relative permeability characteristics. Soc Petrol Eng J 10(01):75–84

Shahverdi H (2012) Characterization of three-phase flow and WAG injection in oil reservoirs. Heriot-Watt University, Edinburgh

Shahverdi H, Sohrabi M (2013) An improved three-phase relative permeability and hysteresis model for the simulation of a water-alternating-gas injection. SPE J 18(05):841–850

Shahverdi H, Sohrabi M (2014) Modeling of cyclic hysteresis of three-phase relative permeability during water-alternating-gas injection. SPE J 20(01):35–48

Shahverdi H, Sohrabi M, Jamiolahmady M (2011) A new algorithm for estimating three-phase relative permeability from unsteady-state core experiments. Transp Porous Media 90(3):911–926

Sigmund P, McCaffery F (1979) An improved unsteady-state procedure for determining the relative permeability characteristics of heterogeneous porous media (includes associated papers 8028 and 8777). Soc Petrol Eng J 19(01):15–28

Sinha PK, Wang C-Y (2007) Pore-network modeling of liquid water transport in gas diffusion layer of a polymer electrolyte fuel cell. Electrochim Acta 52(28):7936–7945

Skjaeveland S, Siqveland L, Kjosavik A, Hammervold W, Virnovsky G (1998) Capillary pressure correlation for mixed-wet reservoirs. SPE India Oil and Gas conference and exhibition. Society of Petroleum Engineers

Sola BS, Rashidi F, Babadagli T (2007) Temperature effects on the heavy oil/water relative permeabilities of carbonate rocks. J Petrol Sci Eng 59(1):27–42

Watson A, Richmond P, Kerig P, Tao T (1988) A regression-based method for estimating relative permeabilities from displacement experiments. SPE Reserv Eng 3(03):953–958

Xiong Q, Baychev TG, Jivkov AP (2016) Review of pore network modelling of porous media: experimental characterisations, network constructions and applications to reactive transport. J Contam Hydrol 192:101–117

Spearing M, Cable A, Element D, Dabbour Y, Al Massabi A, Negahban S, Kalam Z Case study of water flood relative permeability measurements for two middle eastern carbonate reservoirs

Yaralidarani M, Shahverdi H (2016) An improved ant colony optimization (ACO) technique for estimation of flow functions (k_r and P_c) from core-flood experiments. J Nat Gas Sci Eng 33:624–633